Journal of Integrative Agriculture 2026, 25(9): 3904–3916

Available online at ScienceDirect

Journal of Integrative Agriculture

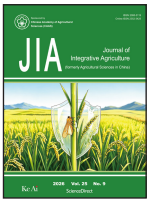

RESEARCH ARTICLE

Impacts of *Bacillus velezensis* inoculation on exogenous organic carbon mineralization and bacterial community composition in fumigated continuous-cropping obstacle soils

Yixian Liu[1, 2], Runa Zhang[1, 2], Shuai Ding[1, 2#], Shuang Wang[1, 2], Liang Wei[1, 2], Cuiyan Wu[3], Wensheng Fang[4], Qiuxia Wang[4], Dongdong Yan[4], Aocheng Cao[4], Jianping Chen[1, 2], Tida Ge[1, 2], Zhenke Zhu[1, 2#]

[1] *State Key Laboratory for Quality and Safety of Agro-products/Key Laboratory of Biotechnology in Plant Protection of Ministry of Agriculture and Rural Affairs/Key Laboratory of Green Plant Protection of Zhejiang Province/Institute of Plant Virology, Ningbo University, Ningbo 315211, China*

[2] *International Science and Technology Cooperation Base for the Regulation of Soil Biological Functions and One Health of Zhejiang Province, Ningbo University, Ningbo 315211, China*

[3] *School of Materials and Chemical Engineering, Ningbo University of Technology, Ningbo 315211, China*

[4] *Institute of Plant Protection, Chinese Academy of Agricultural Sciences, Beijing 100193, China*

Highlights

- Dazomet and dimethyl disulfide fumigation suppress exogenous organic carbon (C) mineralization.
- *Bacillus velezensis* inoculation restores C mineralization and increases microbial respiration.
- *Bacillus velezensis* reshapes bacterial communities and strengthens bacterial interactions.
- Microbial remediation can restore soil function in intensive agricultural systems.

Abstract

Chemical fumigants such as dazomet (DZ) and dimethyl disulfide (DMDS) effectively suppress soil-borne pathogens but there is uncertainty regarding the restoration of soil ecological functions in continuous cropping obstacles after fumigation, such as microbe-mediated organic carbon cycling. However, the mechanism by which microbial remediation measures enhance carbon mineralization activity after soil fumigation remains unclear. In this study, we conducted microcosm experiments to investigate the impacts of *Bacillus velezensis* inoculation on exogenous organic carbon (EOC) mineralization and bacterial community composition and interactions following chemical fumigation. Relative to fumigation alone, *B. velezensis* addition increased cumulative EOC mineralization by 27% in DZ-treated soils and by 22% in DMDS-treated soils. This enhancement was associated with the enrichment of core taxa and keystone species, which collectively increased microbial activity. Structural equation modeling further confirmed that core taxa (OTU56, belonging to *Bacillus*) induced positive interactions with indigenous species, which drove the observed enhancement in EOC mineralization. We conclude that *B. velezensis* facilitates the rapid recovery of soil carbon mineralization after fumigation by selectively reshaping the bacterial community and strengthening bacterial cooperative networks. This work provides a mechanistic framework for microbially driven ecological restoration of fumigant-impacted continuous-cropping obstacle soils and informs the development of sustainable soil-management practices in chemically challenged agroecosystems.

Keywords: continuous cropping obstacles, chemical fumigation, *B. velezensis*, microbial community structure, organic carbon mineralization

1. Introduction

The long-term monoculture of economic crops often leads to a proliferation of soil-borne pathogens and a decline in soil physico-chemical and biological properties, resulting in severe yield losses of more than 50%, which threaten the sustainability of intensive agricultural systems (Deng *et al.* 2021). Chemical fumigation with broad-spectrum agents, such as dazomet (DZ) and dimethyl disulfide (DMDS), is

Received 8 August 2025; Received in revised form 23 October 2025; Accepted 12 December 2025; Available online 2 January 2026
Yixian Li, E-mail: 2311130026@nbu.edu.cn; #Correspondence Shuai Ding, E-mail: dingshuai@nbu.edu.cn; Zhenke Zhu, E-mail: zhuzhenke@nbu.edu.cn

doi: 10.1016/j.jia.2025.12.076

commonly employed to alleviate these continuous cropping obstacles by effectively eliminating pathogenic organisms (Castellano-Hinojosa *et al.* 2022; Schulte-Uebbing *et al.* 2022). However, chemical fumigation also reduces soil microbial diversity, posing challenges to the targeted restoration of soil ecological functions in continuous cropping obstacles (Xiong *et al.* 2024).

The biogeochemical carbon cycle constitutes a key component of soil ecosystem functionality. Microbial abundance and diversity are fundamental to soil health, as their activities underpin critical processes like organic matter decomposition, which directly influences soil fertility and nutrient availability (Ibekwe *et al.* 2001; Bissett *et al.* 2013). Soil microbial communities exhibit dynamic changes in response to environmental disturbances, such as chemical fumigation, which significantly alter the microbial community composition, reduce network complexity, and impair functional potential (Castellano-Hinojosa *et al.* 2022). Specifically, fumigation significantly reduces the abundance of key functional microbial groups, including *Bacillus*, *Pseudomonas*, and arbuscular mycorrhizal fungi. Such declines can disrupt microbial-mediated residue decomposition processes, ultimately impairing the organic carbon sequestration capacity of the soil (Cao *et al.* 2024; Philippot *et al.* 2024). Recent evidence has further suggested that a decrease in microbial abundance and metabolic activity after fumigation slows down the exogenous organic carbon (EOC) mineralization, which is a direct indicator of microbial activity (Liang *et al.* 2017; Abs *et al.* 2024). Despite increasing recognition of the ecological consequences of soil fumigation, current research focuses on its effects on pathogen suppression and crop productivity, and neglects the impacts on soil microbial communities and carbon mineralization activity (Yan *et al.* 2025). This knowledge gap hinders the rapid restoration of microbial C cycling functions in fumigated continuous cropping soils. Therefore, exploring effective strategies for microbial ecological restoration post-fumigation has scientific and practical implications.

Various soil amendments (e.g., silicate minerals, biochar, organic fertilizers) are employed after chemical fumigation to restore impaired microbial diversity and ecological functions (Fang *et al.* 2020). These non-biological amendments primarily improve soil physicochemical parameters and promote microbial recolonization (Chen *et al.* 2025; Jiang *et al.* 2025). In contrast, biologically active amendments, especially microbial inoculants, may offer a more direct and efficient pathway for microbial community and function reconstruction (Zargar *et al.* 2022). *Bacillus* spp. has exhibited excellent capabilities in resisting abiotic stress (Li *et al.* 2025), suppressing pathogens, and promoting soil carbon cycling (Wang *et al.* 2018). For example, *Bacillus velezensis* can produce extracellular enzymes and secondary metabolites to enhance microbial activity and modulate community interactions, thereby demonstrating potential as a viable inoculant for post-fumigation recovery (Mosela *et al.* 2022). However, the mechanisms by which *Bacillus* inoculation restores carbon cycling functions (particularly soil organic carbon (SOC) mineralization) in fumigated continuous cropping soils remain largely unknown. Specifically, whether *Bacillus* inoculation enhances carbon mineralization through increasing microbial metabolic activity or restructuring the microbial community and interactions remains unclear.

To investigate these gaps, we explored the role of *B. velezensis* in restoring EOC mineralization and bacterial community structure in chemically fumigated continuous cropping soils. Using a controlled microcosm approach, we examined the impacts of *B. velezensis* inoculation following DZ and DMDS fumigation on bacterial diversity, co-occurrence network properties, and carbon mineralization dynamics. We hypothesized that: (i) *Bacillus velezensis* inoculation increases the EOC mineralization rate in fumigated soils, and (ii) this enhancement is driven by the restructuring of bacterial community composition and the promotion of cooperative interactions among keystone taxa. Our findings offer mechanistic insight into microbe-mediated carbon cycling recovery and provide a theoretical foundation for integrating microbial amendments into sustainable fumigation and soil restoration strategies.

2. Materials and methods

2.1. Site description and soil sampling

Soil sampling was conducted in March 2024 from a greenhouse under continuous tomato monocropping in Cixi City, Zhejiang Province, China (30°16´N, 121°14´E). The study site has a climate characterized by an annual average temperature of 16.0°C and precipitation of 1,272 mm. Prior to collection, visible stones and plant debris were manually removed from the soil surface. The topsoil (0–20 cm) was carefully collected, sieved through a 2-mm mesh, homogenized, and stored at 4°C for subsequent incubation experiments. Soil physical and chemical properties were analyzed, including pH, electrical conductivity (EC), SOC, dissolved organic carbon (DOC), ammonium nitrogen (NH_4^+), nitrate nitrogen (NO_3^-), and available phosphorus (Olsen-P). The basic soil properties were as follows: SOC, 12.8 g kg^{-1}; DOC, 78.7 mg kg^{-1}; NH_4^+, 1.0 mg kg^{-1}; NO_3^-, 160.0 mg kg^{-1}; Olsen P, 94.5 mg kg^{-1}; EC, 640 μs cm^{-1}; and pH 7.5 (1:2.5 w/v).

2.2. Soil chemical fumigation and *Bacillus* inoculation

Soil samples were adjusted to 20% moisture content and equilibrated for one week. Before fumigation, each 50-g soil sample was placed in black plastic containers and mixed with DZ (180 mg kg^{-1} dry soil) or DMDS (128 mg kg^{-1} dry soil). The dosage was determined according to the recommended field usage (375–450 kg ha^{-1}), and control samples received no fumigant (Prider and Williams 2014; Yan *et al.* 2019). All containers were thoroughly mixed, sealed, and held for 10 days to allow the fumigants to react. Following this incubation, soils were aired in a fume hood for 10 days to ensure complete volatilization of residual chemicals. Previous studies have reported the complete removal of residual fumigant in the soil following this procedure (Dungan *et al.* 2003).

The recovery of soil organic carbon mineralization following fumigation was assessed *via* an incubation experiment after fumigation based on the following six treatments (with each

performed in triplicate): (1) unfumigated continuous cropping soil+^{13}C-root exudates (CKR); (2) unfumigated continuous cropping soil+^{13}C-root exudates+*B. velezensis* (CKRB): (3) DZ-fumigated continuous cropping soil+^{13}C-root exudates (DZR); (4) DZ-fumigated continuous cropping soil+^{13}C-root exudates+*B. velezensis* (DZRB); (5) DMDS-fumigated continuous cropping soil+^{13}C-root exudates (DMDSR); and (6) DMDS-fumigated continuous cropping soil+^{13}C-root exudates+*B. velezensis* (DMDSRB). In this study, the suffixes "RB" and "R" indicate treatments with and without *B. velezensis* inoculation, respectively. To simulate root exudation during the crop growth period after fumigation, we added a ^{13}C-labelled substrate mixture (3.0 atom% ^{13}C; Cambridge Isotope Laboratories, Tewksbury, MA, USA) consisting of glucose, oxalic acid, and alanine in a 65:30:5 mass ratio at a carbon input equivalent to 100% of the soil microbial biomass C: 168.3 mg C kg^{-1} for control soils, 140.4 mg C kg^{-1} for DZ-treated soils, and 71.1 mg C kg^{-1} for DMDS-treated soils (Chowdhury *et al.* 2014; Cui *et al.* 2020). In treatments with inoculation, *B. velezensis* was added at 10^7 CFU g^{-1} dry soil (*via* a single inoculation on the 0th day of incubation). Each 50-g soil sample was placed in a 250 mL plastic bottle prepared according to the specific treatment conditions, then incubated in the dark at 25°C. Destructive sampling was performed on days 1, 3, 10, and 30 to measure a suite of soil properties, encompassing physicochemical characteristics, biochemical processes, and microbial composition.

2.3. Sampling and analysis

Gas sampling and analysis Gas samples were collected periodically (on days 1, 2, 4, 6, 8, 10, 12, 14, 16, 20, 25, and 30) to monitor gas flux dynamics. Each soil sample was partitioned into two aliquots for distinct analyses: one for measuring CO_2 concentration and one for analyzing $^{13}CO_2$ abundance. A gas chromatograph (7890 B, Agilent Technologies, California, USA) was used to measure CO_2 concentration, and an isotope ratio mass spectrometer with a GasBench (Picarro G2201-I, Picarro, Silicon Valley, USA) was employed to determine the ^{13}C isotope ratio.

The incorporation of exogenous ^{13}C into $^{13}CO_2$ was quantified using the equation:

$$\text{excess}^{13}CO_{2\text{sample}}=\frac{(\text{atom\% }^{13}CO_2)_L-(\text{atom\% }^{13}CO_2)_{UL}}{100}\times CO_{2\text{sample}} \quad (1)$$

where (atom% $^{13}CO_2)_L$ represents the $^{13}CO_2$ atom percentage in the labeled reference, (atom% $^{13}CO_2)_{UL}$ represents that in the unlabeled reference, and $CO_{2sample}$ indicates the CO_2-C measured in the experimental sample. Cumulative EOC mineralization was quantified by summing the total CO_2-C evolved during each incubation interval over the entire experimental period. The cumulative mineralization rate (%) was determined as the ratio of the total mineralized C to the initial amount of EOC added. Methane (CH_4) emissions from the soil were deemed negligible (contributing less than 1% of the total CO_2 equivalents) and were excluded from the total greenhouse gas emission calculations.

Soil physicochemical properties Measurement of soil pH and EC was performed using a Mettler Toledo Seveneasy pH meter (Mettler Toledo Seveneasy, Greifensee, Switzerland) at soil-to-water ratios of 1:2.5 and 1:5, respectively. For the analysis of DOC, NH_4^+, and NO_3^-, soil samples were extracted with 0.5 mol L^{-1} K_2SO_4, followed by quantification with a total organic carbon (TOC) analyzer (Multi N/C 3100; Analytik Jena, Freistaat Thüringen, Germany) and an AutoAnalyzer continuous flow system (Seal Analytical, Freistaat Thüringen, Germany). Following extraction with 0.5 mol L^{-1} $NaHCO_3$ (pH 8.5), Olsen-P was quantified using the same continuous flow analyzer.

Microbial biomass carbon (MBC) and nitrogen (MBN) were determined by the chloroform fumigation-extraction method (Brookes *et al.* 1985; Wu *et al.* 1990). Two 10 g soil subsamples were processed in parallel: one non-fumigated (extracted directly with 0.5 mol L^{-1} K_2SO_4 at a 1:4 soil-to-solution ratio) and one fumigated (exposed to chloroform for 24 h in the dark before identical extraction). TOC and TON in the extracts were quantified using a TOC analyzer. MBC and MBN were calculated as the difference between fumigated and non-fumigated samples, applying conversion factors of 0.45 and 0.54, respectively.

Enzymatic activity assay We analyzed the activities of extracellular enzymes involved in C cycling (β-glucosidase, β-cellobiohydrolase, β-xylosidase), N cycling (N-acetyl-β-glucosaminidase), and P cycling (alkaline phosphatase) (Sinsabaugh and Follstad Shah 2012; Ge *et al.* 2017). Soil extracts were prepared by suspending fresh soil samples in 0.5 mol L^{-1} $NaHCO_3$ solution. Microplate assays were performed by dispensing 200 µL of the soil extract into each well of a 96-well microplate and adding enzyme-specific 4-methylumbelliferyl substrates. Following a 4-h incubation at 25°C, the reactions were terminated by adding 10 µL of 1 mol L^{-1} NaOH. Fluorescence measurement was performed on a BioTek Synergy H1 microplate reader (Vermont, USA) using excitation/emission wavelengths of 365 and 450 nm. Enzyme activity was calculated and expressed as nmol of 4-methylumbelliferone released per gram of dry soil per hour.

2.4. Partitioning CO_2 sources

The stable carbon isotope ratios of glucose and CO_2 were reported relative to the Pee Dee Belemnite (PDB) standard using δ (‰) notation and subsequently converted to atomic percentages (atom%). The δ^{13}C value was calculated using the following equation:

$$\delta^{13}C=(R_{sample}/\text{Rv-PDB}-1)\times 1{,}000 \quad (2)$$

where the $^{13}C/^{12}C$ ratios of the sample and the Vienna PDB standard are represented by R_{sample} and Rv-PDB, respectively.

The quantities of ^{13}C-glucose derived from DOC and MBC in the glucose-amended treatments, as well as the quantities of $^{13}CO_2$ efflux, were determined by applying the following equation:

$$CO_{2glu}=\frac{(\text{atom\% }^{13}CO_{soil}-\text{atom\% }^{13}C_{total}}{(\text{atom\% }^{13}C_{soil}-\text{atom\% }^{13}C_{glu}}\times CO_{2total} \quad (3)$$

CO_{2glu}, which represents the fraction of CO_2 derived from added glucose, was quantified using an end member mixing model. The model incorporated the atomic percentage of ^{13}C in CO_2 from the glucose-amended samples (atom% $^{13}C_{glu}$) and

from the control (atom% $^{13}C_{soil}$), whereas CO_{2total} corresponds to the total CO_2 produced during glucose treatment (Philippot *et al.* 2024).

2.5. Carbon use efficiency (CUE) and microbial metabolic entropy calculations

CUE was calculated according to the following equation (Del Giorgio and Cole 1998):

$$CUE=^{13}C\text{-}MBC/(^{13}C\text{-}MBC+^{13}C\text{-}CO_2) \quad (4)$$

The microbial metabolic quotient (qCO_2), where ^{13}C-MBC is glucose-derived microbial biomass carbon and ^{13}C-CO_2 is glucose-originated CO_2, was calculated using the equation below:

$$qCO_2\ (\mu g\ CO_2\text{-}C\ h^{-1}\ mg^{-1}\ MBC)=r/MBC \quad (5)$$

where r is the respiration rate (μg CO_2-C h^{-1}) and MBC the microbial biomass carbon (mg). CUE and qCO_2 quantify the efficiency of microbial biomass carbon utilization and the specific respiration rate, respectively, making them essential metrics for assessing microbial metabolism and soil carbon dynamics.

2.6. DNA extraction and microbial community analysis

To prevent microbial death caused by fumigation from affecting DNA sequencing, we blocked the residual DNA with propidium monoazide before extracting the DNA to prevent amplification (Carini *et al.* 2016). We placed 0.3 g of soil in a plastic transparent tube and added 600 μL of phosphate buffer solution (pH=7.4). Propidium monoazide was added to the sample in the dark at a final concentration of 40 μL L^{-1} (Wei *et al.* 2021). The plastic transparent tube was vortexed in the dark for 4 min, then vortexed under a 650-W halogen lamp for 4 min; this process was repeated for four cycles. To ensure quality for downstream analysis, soil DNA was extracted using the Easy PowerSoil Kit (Qiagen, Germany) according to the manufacturer's instructions. All extracted DNA exhibited spectrophotometric concentrations of 10–40 ng μL^{-1} and 260/280 ratios of 1.8–2.0.

Using primers 515F (5′-GTGCCAGCMGCCGCGGTAA-3′) and 806R (5′-GGACTACHVGGGTWTCTAAT-3′), the V4–V5 region of the bacterial 16S rRNA gene was amplified as described by Walters *et al.* (2016). Sequencing of the amplicons was conducted using the Illumina MiSeq PE250 platform (Illumina, USA) at Novogene Bioinformatics Technology Co., Ltd. (Tianjin, China). Raw reads were processed using the QIIME 2 pipeline, with demultiplexing and quality filtering performed *via* the q2-demux plugin. Denoising and chimera removal were performed using DADA2 to generate high-quality sequences (Callahan *et al.* 2016). An OTU table was constructed for microbial community analysis following sequence classification against the SILVA database and clustering at 97% similarity into 33023 OTUs (Quast *et al.* 2012).

2.7. Bacterial strain and identification

Bacillus velezensis NBU-X21, isolated from dryland agricultural soil, has been deposited in China General Microbiological Culture Collection Center (CGMCC No. 27616; deposited June 12, 2023). For molecular identification, the genomic DNA of strain NBU-X21 was amplified with the universal 16S rDNA primers 27F and 1492R. The 25 μL PCR mixture contained 1.0 μL of DNA template (20 ng μL^{-1}), 1.5 μL of each primer, 7.0 μL of PCR Mix, and ddH_2O to volume. The thermal cycling protocol comprised initial denaturation at 95°C for 5 min; 30 cycles of 95°C for 30 s, 58°C for 30 s, and 72°C for 100 s; and a final extension at 72°C for 7 min. The resulting amplicons were purified and sequenced, and the sequences were analyzed *via* BLAST against the NCBI database. A phylogenetic tree constructed using MEGA software, combined with physiological and biochemical characterization, confirmed the identity of strain NBU-X21 as *B. velezensis*.

2.8. Identification of core species

The identification of core species was performed using an integrated approach that combined network topology and differential abundance analyses. A microbial co-occurrence network was first constructed based on OTU correlations using the "igraph" package in R. Keystone species were determined by Zi-Pi analysis. Based on their topological features, nodes were classified as: module hubs (Zi≥2.5, Pi<0.62), connectors (Zi<2.5, Pi≥0.62), or network hubs (Zi≥2.5, Pi≥0.62). All such nodes were defined as keystone species because of their crucial roles in maintaining network structure. To focus on treatment-specific keystones, OTUs shared between the DZ and CK groups were removed using Venn diagram analysis, retaining only DZ-specific taxa. Independently, differential species under RB treatment were identified, and OTUs that were DZ-specific keystones and RB-responsive differential species were defined as core species, representing taxa that are structurally important within the microbial network and responsive to treatment interventions.

2.9. Statistical analyses

Multiple regression analyses were conducted using the R package "MuMIn" to evaluate the effects of different environmental variables (SOC, DOC, β-glucosidase, β-cellobiohydrolase, MBC, pH, EC, Olsen P, NH_4^+, NO_3^-, richness, Shannon index, and abundance) on EOC mineralization (Appendix A). The best-fitting model was selected from all-subsets regression based on the lowest akaike information criterion (AIC) value, identifying the most influential predictors. Data analysis was performed in R. Alpha diversity and principal coordinate analysis (PCoA) based on Bray-Curtis distance were conducted using the "vegan" package. Differential species were identified by linear discriminant analysis effect size (LEfSe) with the "microeco" package; correlation analysis between mineralization rates and physicochemical indicators, as well as Venn diagrams, were implemented with "pheatmap" and "venn", respectively. A co-occurrence network was visualized in Gephi 0.9.2, with Zi-Pi analysis performed *via* the "BiocManager" ecosystem. The relative contributions of factors to carbon mineralization were quantified using structural equation modeling in "piecewiseSEM". Analysis of variance was applied to determine statistical significance, with levels denoted as

*, P<0.05, **, P<0.01, and ***, P<0.001.

3. Results

3.1. EOC mineralization

EOC mineralization was substantially suppressed by chemical fumigation but subsequently recovered following *B. velezensis* inoculation. Specifically, cumulative EOC mineralization in DZ-treated soils (DZR) and DMDS-treated soils (DMDSR) decreased by 22.2 and 32.0% relative to the non-fumigated control (CKR), respectively. In contrast, *B. velezensis* application increased EOC mineralization by 22.2 and 15.9% (in DZRB and DMDSRB compared to DZR and DMDSR, respectively) (Fig. 1). Notably, DZRB treatment restored EOC mineralization to control levels, whereas CKRB showed no significant difference from CKR (Fig. 1).

The microbial C metabolic characteristics were similar to the EOC mineralization results. On day 1, CUE in DZRB and DMDSRB declined by 42.2 and 46.3%, respectively, compared with that in DZR and DMDSR (Appendix B). Concurrently, qCO_2 in DZRB and DMDSRB increased by 46.5 and 183.2%, respectively, compared to that in DZR and DMDSR (Appendix B). *Bacillus velezensis* inoculation effectively alleviated the inhibitory effects of chemical fumigation on soil carbon mineralization, promoting the recovery of microbial metabolic activity and carbon turnover efficiency.

3.2. Bacterial diversity and community composition

Chemical fumigation significantly altered soil bacterial diversity and community structure. DZ and DMDS treatments reduced the bacterial richness from that in the non-fumigated control (Fig. 2-A). The addition of *B. velezensis* further decreased the richness in DZ-fumigated continuous cropping soil, but slightly increased the richness in DMDS-fumigated continuous cropping soil. Principal coordinate analysis revealed a clear separation in microbial communities between the fumigated treatment and the control, confirming that fumigation induced a strong shift in microbial community composition (Fig. 2-B).

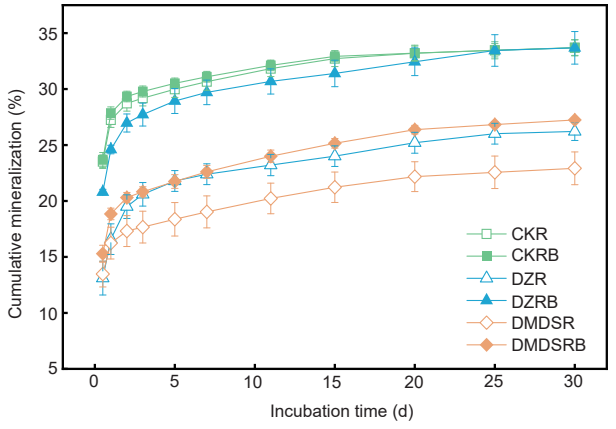

Fig. 1 Effect of *Bacillus* application on relative exogenous organic carbon (EOC) mineralization rates after chemical fumigation. CKR, unfumigated soil+^{13}C-root exudates; CKRB, unfumigated soil+^{13}C-root exudates+*B. velezensis*; DZR, DZ-fumigated soil+^{13}C-root exudates; DZRB, DZ-fumigated soil+^{13}C-root exudates+*B. velezensis*; DMDSR, DMDS-fumigated soil+^{13}C-root exudates; DMDSRB, DMDS-fumigated soil+^{13}C-root exudates+*B. velezensis*. Symbols represent mean values and error bars represent standard errors.

To assess how *B. velezensis* inoculation influenced community recovery, we compared the bacterial community composition and differential species with and without *B. velezensis* addition in fumigated continuous cropping soils. In DZ, Pseudomonadota was the dominant phylum (29–31%), whereas Bacillota accounted for 11–24%. Over time, *B. velezensis* inoculation reduced the relative abundance of Bacillota in DZ soil from 24 to 11% but increased the abundance of Acidobacteriota by 2.6% (Fig. 2-C; Appendix C). In DMDS treatment, Pseudomonadota remained the dominant phylum (Fig. 2-D). However, we observed no significant difference in the abundance of species with and without *Bacillus* inoculation. Overall, these results suggest that *B. velezensis* modulates the recovery of microbial community post-fumigation by selectively enriching taxa associated with organic carbon turnover. Specifically, *B. velezensis* inoculation reshaped the post-fumigation bacterial community structure and promoted the enrichment of functional taxa involved in carbon cycling.

3.3. Factors influencing EOC mineralization

To determine the relative importance of soil properties, microbial diversity, and activity on EOC mineralization, we constructed multiple regression models for fumigated continuous cropping soils with and without *B. velezensis* inoculation. Both models explained a high proportion of the variability in cumulative EOC mineralization (R^2=0.87, without inoculation; R^2=0.88 with inoculation; Fig. 3-A and C).

In both models, microbial activity was the dominant driver, accounting for approximately half of the explained variation (50.2% without *B. velezensis* and 50.8% with *B. velezensis*; Fig. 3-A and C). Microbial diversity, as indicated by the Shannon index, was the second important factor. Notably, the contribution of microbial diversity increased by 8.2% after *B. velezensis* inoculation, indicating that restoration and restructuring of the microbial community explain the enhanced C mineralization. Other soil parameters (e.g., pH, moisture, and nutrient content) together accounted for <25% of cumulative EOC mineralization variability. These results suggest that microbial activity and diversity are the primary determinants of EOC mineralization, with *B. velezensis* inoculation amplifying the role of microbial diversity in driving carbon turnover.

3.4. Microbial co-occurrence network analysis

According to microbial network analysis, DMDS fumigation did not alter the bacterial community composition; therefore, we only describe the results for DZ-treated soils with and without *B. velezensis* inoculation. DZRB treatment increased the number of nodes and edges by 8.5 and 33.9%, respectively, and the proportion of positive correlations by 3.4% relative to DZ treatment alone (Fig. 4-A and B). Network robustness, assessed by the change in connectivity

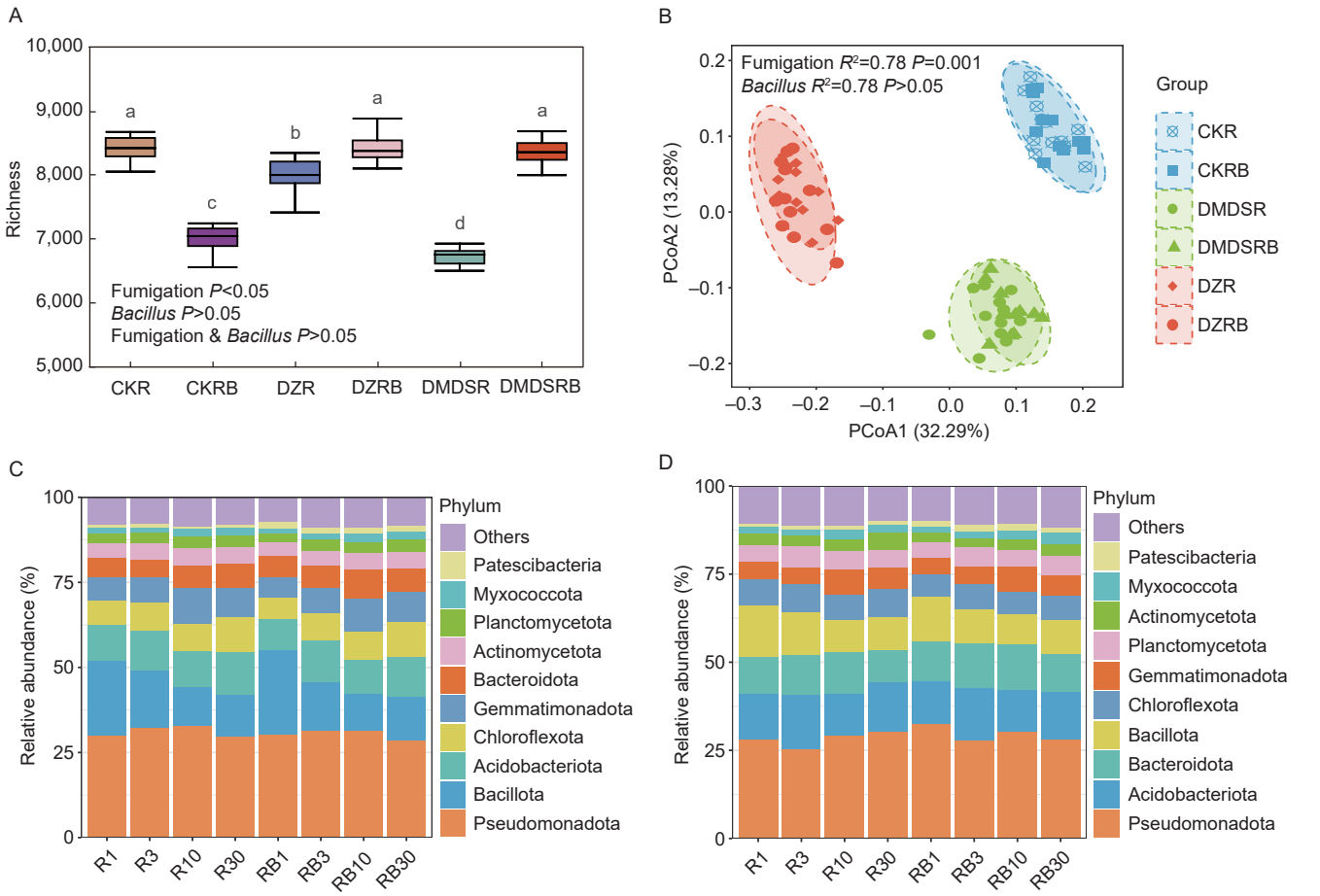

Fig. 2 Bacterial community composition following fumigation. A, effect of different fumigants on richness index and effect of *Bacillus* remediation on the richness index. B, changes in β-diversity under different fumigant treatments and remediation of *Bacillus*. C and D, composition of bacterial phyla in DZ-fumigated (C) and DMDS-fumigated (D) continuous cropping soils with and without *Bacillus* inoculation. CKR, unfumigated soil+^{13}C-root exudates; CKRB, unfumigated soil+^{13}C-root exudates+*B. velezensis*; DZR, DZ-fumigated soil+^{13}C-root exudates; DZRB, DZ-fumigated soil+^{13}C-root exudates+*B. velezensis*; DMDSR, DMDS-fumigated soil+^{13}C-root exudates; DMDSRB, DMDS-fumigated soil+^{13}C-root exudates+*B. velezensis*. R, root exudates; RB, root exudates and *B. velezensis*.

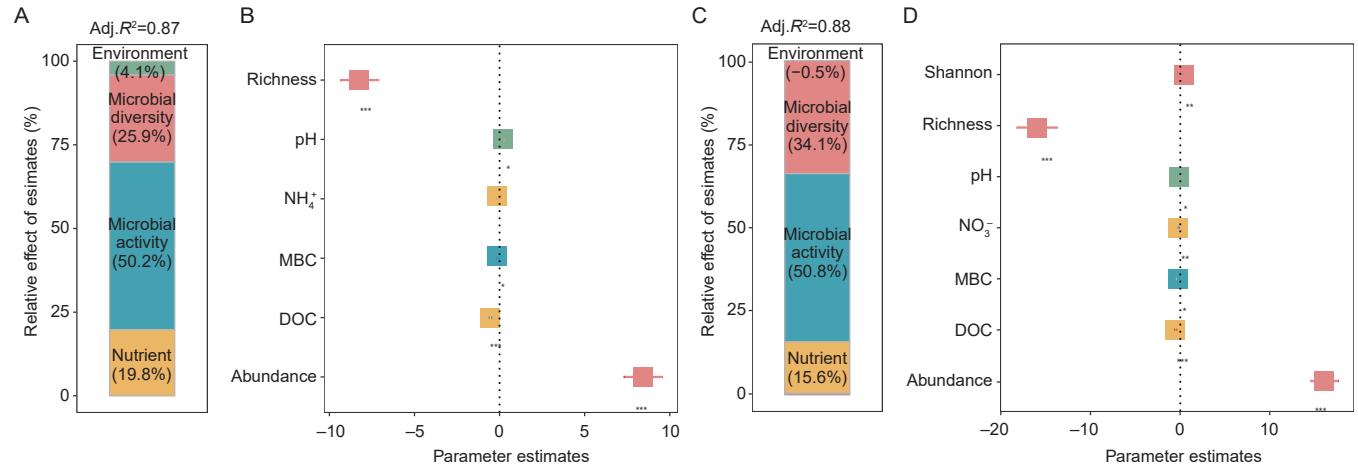

Fig. 3 Relative contributions of multiple predictive factors to exogenous organic carbon (EOC) mineralization rate. A and C, parameter estimates of predictive factors in untreated (A) and *Bacillus*-treated (C) soils. B and D, relative importance of each predictive factor for EOC mineralization, expressed as the percentage of explained variance, for the untreated soil (B) and *Bacillus*-treated soil (D). Predictive factors include: environmental factors (electrical conductivity, pH); microbial diversity factors (richness, Shannon index, species abundance), microbial activity factors (microbial biomass carbon MBC, β-glucosidase, β-cellobiohydrolase), and nutrient factors (SOC, dissolved organic carbon DOC, NH_4^+, NO_3^- and Olsen P). *, P<0.05, **, P<0.01, and ***, P<0.001.

after the random removal of 5–25% of nodes, improved by 1.8–7.1% in DZRB, indicating greater community stability after microbial remediation. Network stability, negative cohesion, and positive cohesion also increased in DZRB (Fig. 4-E–G), further indicating tighter network integration with *Bacillus* inoculation. Next, we identified keystone taxa and conducted module analysis. Modules 2 and 3 contained the most OTU numbers in the DZR and DZRB treatments, respectively (Fig. 4-C and D). Bacillota dominated both modules and occupied 48.0% and 45.8% of the sequences in module 2 (DZR) and module 3 (DZRB), respectively. In addition, the identified keystone taxa, defined by high within-module connectivity (Zi) and between-module links (Pi), were all classified as connectors in the Zi–Pi diagram (Appendix D). *Bacillus velezensis* inoculation enhanced the structural complexity and stability of the fumigated soil microbial network, indicating improved community connectivity and resilience following remediation.

3.5. Correlations between bacterial core species and soil properties

To identify the differential species based on the *B. velezensis*-induced network characteristics, we performed LEfSe analysis for the DZRB co-occurrence network and identified two core OTUs (OTU56, *Ferdinandcohnia*, phylum Bacillota; and OTU181, *Niallia*, phylum Bacillota). However, as OTU181 was observed before and after *Bacillus* inoculation, we focus on OTU56 here (Appendix E). We also observed a significant positive correlation between OTU83 and EOC mineralization (Fig. 5-E). Correlation heat mapping revealed

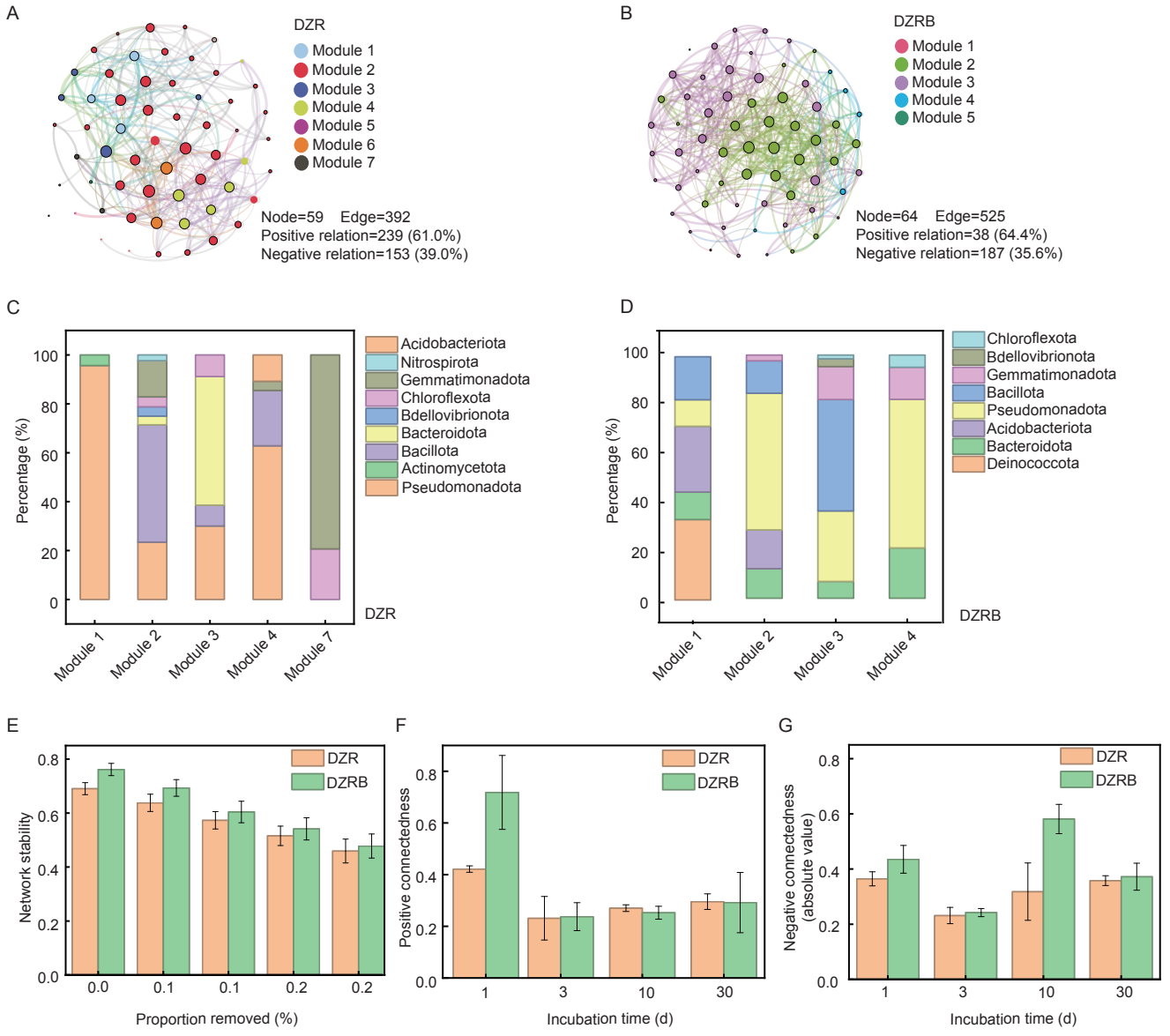

Fig. 4 Bacterial network analysis, species composition of different modules, and Zi–Pi network diagrams after dazomet fumigation. A and B, microbial co-occurrence networks in DZ-fumigated soils without (DZR; A) and with (DZRB; B) *Bacillus* inoculation, respectively. Node size reflects genus-level abundance; colors indicate modules; network parameters (nodes, edges, positive/negative edges) are shown on the right. C and D, phylum-level composition of network modules for DZR (C) and DZRB (D), respectively. E–G, effects of *Bacillus* inoculation on network stability (E), negative cohesion (F), and positive cohesion (G) in DZ-fumigated soils.

that OTU56 was significantly positively correlated with DOC (Fig. 5-A). Furthermore, within the DZRB network, the modules harboring these core taxa (module 3) exhibited strong positive associations with DOC (Fig. 5-B). The correlation between OTU83 and soil physicochemical properties was the opposite to that with OTU56, indicating a significant negative correlation with DOC (Fig. 5-A). In contrast, regression analyses showed that cumulative EOC mineralization was significantly and negatively correlated with the relative abundance of OTU56 (Fig. 5-C), suggesting that a higher module or core taxa dominance corresponds to faster C turnover. In addition, OTU83 displayed a significant positive correlation with the EOC mineralization rate (Fig. 5-D), highlighting its importance in substrate decomposition. The abundance of OTU56 was significantly positively correlated with ^{13}C-substrate use efficiency, whereas OTU83 abundance showed no significant correlation with ^{13}C-substrate use efficiency (Fig. 5-E and F). Despite this, we observed a significant negative correlation between OTU83 and OTU56 (Fig. 5-G and H).

According to network analysis in DZ-fumigated continuous cropping soil without *B. velezensis* (DZR), module 2 was positively associated with DOC but negatively correlated with cumulative EOC mineralization (Appendix F). However, the core taxa (OTU10) were not significantly correlated with either the mineralization rate or physicochemical parameters (Appendix F), indicating that *B. velezensis* inoculation reshaped the entire network structure and also altered key species–function relationships. Overall, *B. velezensis* inoculation modified the microbial network architecture and key taxa composition, thereby enhancing the functional associations between core species and soil carbon dynamics.

3.6. Structural equation modeling of EOC mineralization drivers

To elucidate the impact of *Bacillus* application on EOC mineralization in DZ-fumigated continuous cropping soil, two structural equation models were constructed to quantify the contributions of various factors (Fig. 6-A–D). Both models fit the data well, explaining 95% and 91% of the variance in cumulative EOC mineralization with and without *B. velezensis* inoculation, respectively (Fig. 6-A and C). In soils without *Bacillus* inoculation, soil nutrient availability was the principal positive driver of EOC mineralization (standardized path

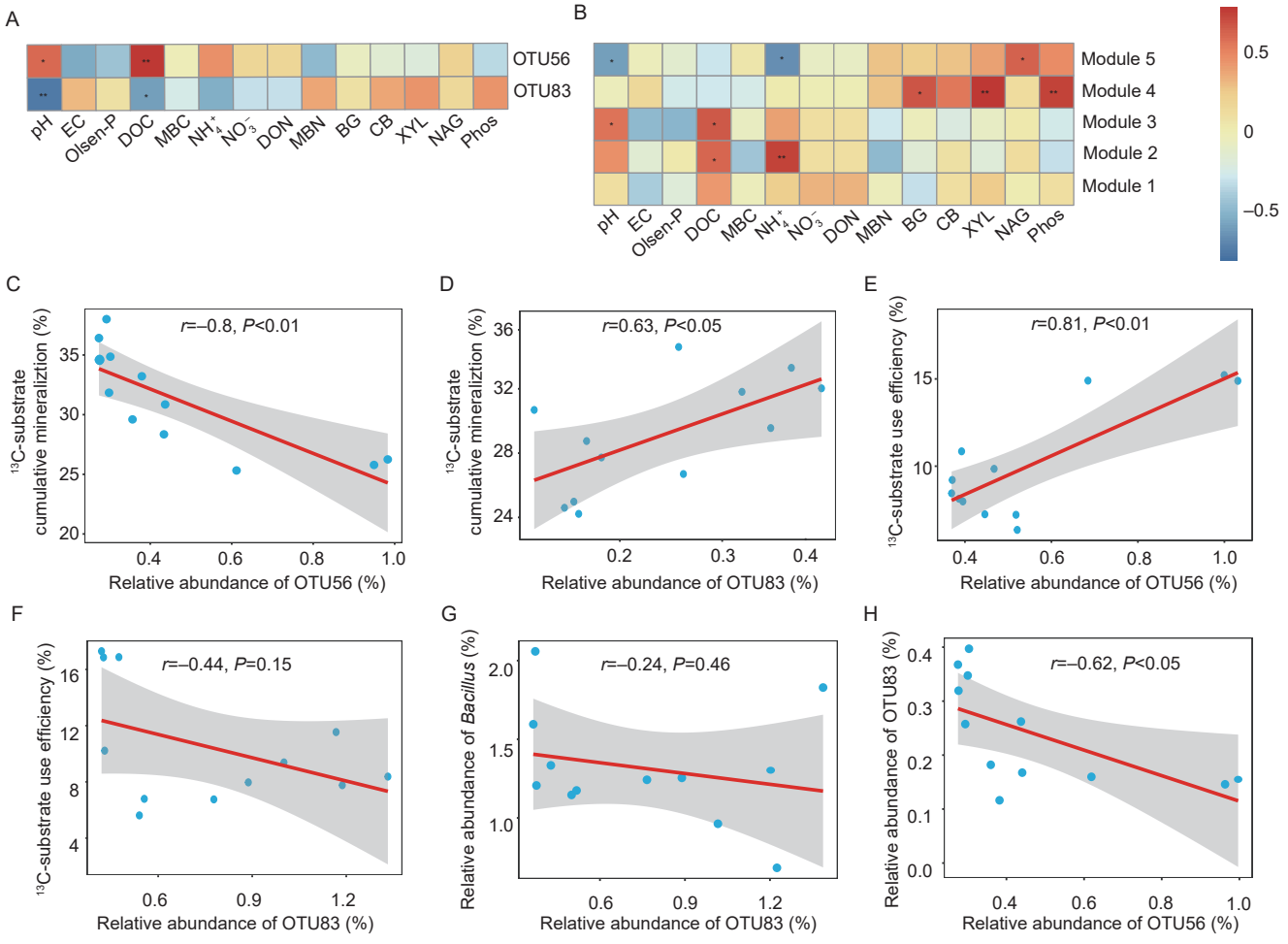

Fig. 5 Correlation analysis and linear regression analysis between core species and key modules and soil physicochemical indicators. EC, electrical conductivity; Olsen-P, Olsen-extractable phosphorus; DOC, dissolved organic carbon; MBC, microbial biomass carbon; DON, dissolved organic nitrogen; MBN, microbial biomass nitrogen; BG, β-1,4-glucosidase; CB, cellobiohydrolase; XYL, β-1,4-xylosidase; NAG, β-1,4-N-acetylglucosaminidase; Phos, phosphatase. *, $P<0.05$, **, $P<0.01$, and ***, $P<0.001$.

coefficient=+0.98); the microbial co-occurrence network also showed a positive contribution (+0.15) (Fig. 6-A). Overall, nutrients had the largest total effect (+0.99) on EOC mineralization (Fig. 6-B), underscoring the importance of substrate supply for driving soil C turnover.

Bacillus velezensis inoculation (DZRB) led to a shift in the relative importance of biotic factors. Nutrients had a strong positive influence (+0.79), but microbial diversity (+0.14) and key taxa abundance (+0.17) had significant positive effects on EOC mineralization (Fig. 6-C). Notably, microbial diversity displayed the greatest total effect (+0.86) among all factors (Fig. 6-D), indicating that restructuring of the bacterial community after inoculation substantially increased C mineralization activity. This transition from negative to positive biotic contributions after *B. velezensis* addition highlights the role of the inoculant in fostering a more functionally cohesive and active microbial assemblage, enhancing soil C cycling beyond that achievable through abiotic recovery alone.

4. Discussion

4.1. *Bacillus velezensis* restores fumigation-suppressed soil microbial activity

Chemical fumigation with DZ and DMDS sharply inhibited EOC mineralization (Fig. 1), confirming that broad-spectrum fumigants disrupt microbial-mediated C turnover (Sennett *et al.* 2022). In our study, cumulative EOC mineralization declined by 22.2% and 32.0% under DZ- and DMDS-fumigated treatments, which aligns with previous reports of reduced soil CO_2 emissions and impaired substrate degradation following fumigation (Sennett *et al.* 2022). The difference in mineralization caused by the two fumigants may be attributed to their different fumigation targets. DMDS tends to inhibit nematodes and fungi, whereas DZ exerts stronger inhibition on bacteria (Yan *et al.* 2025).

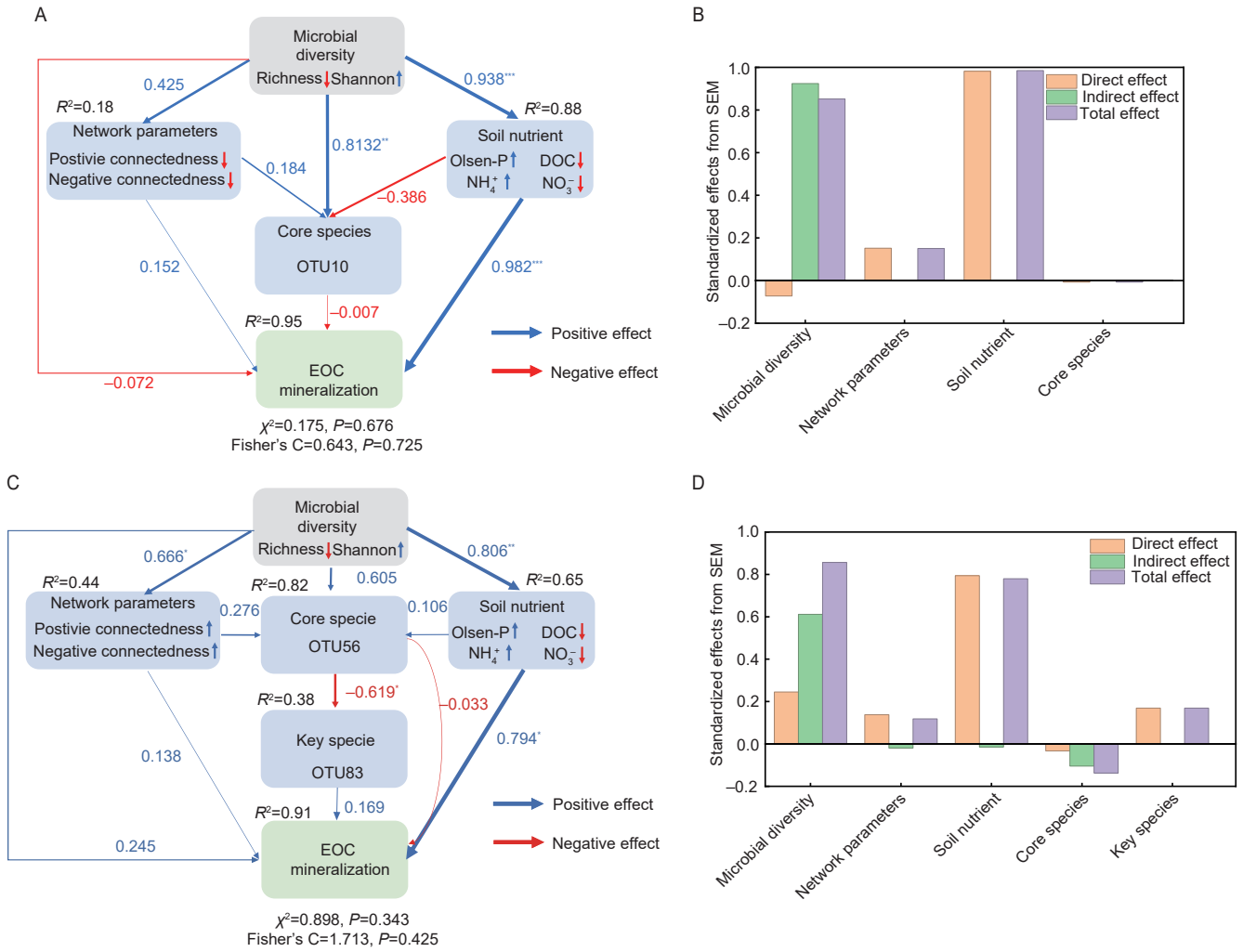

Fig. 6 Structural equation modeling (SEM) of the multivariate effects of environmental factors on exogenous organic carbon (EOC) mineralization. A and C, the total effects of biotic and abiotic factors on exogenous organic carbon (EOC) mineralization in dazomet (DZ)-fumigated soils without (A) and with (C) *Bacillus* inoculation, respectively. B and D, the corresponding direct, indirect, and total effects for the non-inoculated (B) and inoculated (D) treatments, respectively. Path coefficients represent the magnitude of influence; blue and red paths indicate positive and negative effects, respectively. R^2 represents the proportion of variance explained for each variable. Network factors include both positive and negative connectedness; microbial diversity factors include richness and Shannon index; nutrient factors include NO_3^-, DOC, NH_4^+, and Olsen-P. Total effect represents the sum of direct and indirect effects.

Inoculation with *B. velezensis* post-fumigation restored the C mineralization activity; specifically, DZRB treatment restored EOC mineralization to control levels, whereas DMDSRB treatment only recovered 15.9% of EOC mineralization activity (Fig. 1).

In the regression and structural equation modeling (Figs. 3 and 6), microbial activity explained over 50% of EOC mineralization changes, whereas the remaining portion was explained by microbial diversity and soil nutrients (Hui *et al.* 2018; Shu *et al.* 2023). Notably, the contribution of microbial diversity increased from 25.9% in fumigated continuous cropping soils to 34.1% following *Bacillus* inoculation, indicating that the role of community composition becomes increasingly critical (Zhu *et al.* 2018; Wu *et al.* 2026). Together, these results demonstrate that *B. velezensis* accelerates the recovery of C mineralization functions by simultaneously enhancing microbial mineralization rates and reshaping the community structure (Fig. 7).

4.2. *Bacillus velezensis* mediates the restructuring of soil bacterial communities and interactions among keystone taxa

Chemical fumigation with DZ and DMDS significantly reduced bacterial richness and altered community composition (Fig. 2-A), consistent with previous findings that broad-spectrum fumigants simplify microbial assemblages and disrupt key functional groups (Fang *et al.* 2020). This decline in richness reflects the strong selective pressure of fumigation, which eliminates sensitive taxa while allowing resistant or opportunistic species to persist. In DZ-fumigated continuous cropping soils, inoculation with *B. velezensis* further reduced richness (Fig. 2-A), likely by occupying ecological niches and promoting competitive exclusion of certain indigenous bacteria. Notably, this treatment selectively enriched taxa involved in carbon turnover, with *Acidobacteriota* increasing by 2.6% (Fig. 2-C; Appendix C). *Acidobacteriota* harbor genes encoding enzymes capable of degrading complex carbohydrate polymers (Kalam *et al.* 2020). Together, these phyla contribute to carbon mineralization, suggesting that *B. velezensis* promotes C mineralization by selectively enhancing the abundance of efficient decomposers. These shifts indicate that fumigation combined with targeted microbial inoculation can restructure microbial communities toward functionally active but specialized assemblages, potentially influencing soil carbon processing and nutrient dynamics. Concurrently, the proportion of *Pseudomonas* declined, reflecting antagonistic interactions, as *B. velezensis* secretes lipopeptides that suppress competing *Proteobacteria* (Mawarda *et al.* 2022; Pan *et al.* 2025). In DMDS-treated soils, *Bacillus*-mediated remediation did not significantly affect species abundance, possibly because DMDS primarily targets fungi and nematodes and has a relatively smaller impact on bacterial populations (Yan *et al.* 2025). This selective reshaping of the community structure underpins the importance of accelerated EOC turnover.

Network analysis further revealed that *B. velezensis* enhanced the complexity and cooperation of bacterial interactions in DZ soils (Fig. 4). Compared to fumigation alone, the network of DZ-fumigated soils with *Bacillus* inoculation treatment (DZRB) exhibited 8.5% more nodes, 33.9% more edges, and a 3.4% increase in positive correlations. These features indicate a more integrated and resilient microbial community (Zhao *et al.* 2022; Guo *et al.* 2024). Random node-removal tests demonstrated 1.8%–7.1% greater robustness, indicating that inoculation with *B. velezensis* stabilizes the community structure under perturbation (Trabelsi and Mhamdi 2013; Zegeye *et al.* 2019). Moreover, key "connector" OTUs spanned multiple modules (Appendix D), indicating that *B. velezensis* fosters cross-taxon linkages rather than isolated clusters. The increase in *Bacillota* keystone OTUs from 16.7 to 27.4% after inoculation further emphasized that *B. velezensis* recruits more core decomposers. By combining LEfSe and co-occurrence analyses, we identified two core species (OTU56: *Ferdinandcohnia* and OTU181: *Niallia*) that were uniquely enriched after *B. velezensis* inoculation (Appendix G). OTU56 showed strong positive correlations with DOC

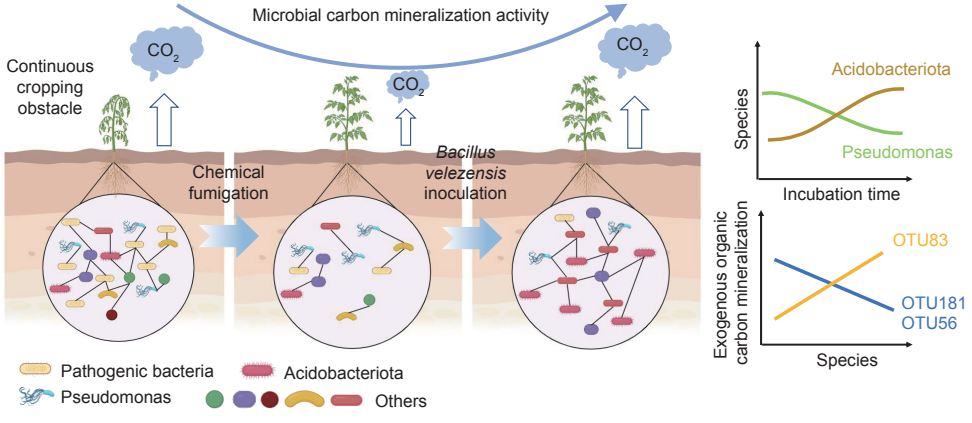

Fig. 7 Conceptual framework showing the effect of *Bacillus velezensis* inoculation on microbial communities and organic carbon mineralization in fumigated soil. Fumigation suppresses exogenous carbon mineralization and decreases bacterial abundance and weakens their interactions in soil. The subsequent addition of *B. velezensis* restored the external carbon mineralization ability, increased the abundance of soil bacteria, and strengthened bacteria interactions.

but negative correlations with cumulative EOC mineralization (Fig. 5-A and C), suggesting that the proliferation of *B. velezensis* accelerates substrate turnover and lowers residual C pools. In contrast, the core taxa in fumigation-only soils (OTU10) showed no significant link to C dynamics, highlighting that *B. velezensis* inoculation creates novel functional associations between keystones and ecosystem processes (Sun *et al.* 2022). Finally, a positive correlation between OTU83 (*Cavicella*) and ^{13}C-substrate mineralization rates (Fig. 5-D) underscored how inoculation selectively amplifies indigenous decomposers beyond the inoculant itself. Together, these findings demonstrate that *B. velezensis* modifies post-fumigation bacterial communities by (i) selectively enriching efficient decomposers, (ii) suppressing competitors, and (iii) reorganizing the network structure to strengthen cooperative interactions among keystone taxa (Fig. 7).

4.3. *Bacillus velezensis* inoculation increases exogenous organic carbon mineralization *via* interaction with indigenous microorganisms

Chemical fumigation impaired soil EOC mineralization mainly by reducing bacterial diversity and altering community composition, which diminished the overall microbial metabolic capacity (Fig. 2-A). In contrast, inoculation with *B. velezensis* rapidly restored the respiration rates (Fig. 1) and reconfigured the community structure and network (Figs. 3 and 6), thereby driving elevated EOC mineralization.

By orchestrating community-wide diversity restructuring, targeted enrichment of essential decomposers, and comprehensive network reconfiguration, *B. velezensis* markedly accelerated soil C mineralization through an integrated mechanism. First, the contribution of microorganisms to mineralization increases after inoculation. In detail, meta-analyses have reported a 41% decline in CO_2 efflux following diversity reduction (Nielsen *et al.* 2011; de Graaff *et al.* 2015). The model of unfumigated soils showed a modest negative effect of diversity loss on EOC mineralization (path coefficient=–0.07; Fig. 6-C). Upon *B. velezensis* addition, changes in diversity exerted a strong positive effect (+0.24; Fig. 6-C), demonstrating that selective reassembly around efficient decomposers can compensate for initial losses and amplify C cycling rates (Malik *et al.* 2018; Liu *et al.* 2025). Second, enrichment of core decomposers promotes rapid turnover of the substrate (Zhu *et al.* 2022; Liang *et al.* 2024). In detail, LEfSe and network analysis identified a highly connected taxa (OTU56, *Ferdinandcohnia*), whose abundance is positively correlated with DOC but negatively correlated with cumulative EOC mineralization (Fig. 5). These core taxa may have specialized metabolic capabilities for degrading organic carbon. Moreover, OTU56 further induces the enrichment of key species OTU83 (Fig. 5-H), which is beneficial for C mineralization (Fig. 5-D). Therefore, *B. velezensis* created a streamlined alliance for optimizing C dioxide production through targeted enrichment (Qiao *et al.* 2024). Third, network reorganization underpins cooperative interactions. In detail, inoculation increased network complexity (nodes=8.5%, edges=33.9%) and the share of positive interaction correlations (3.4%; Fig. 4-A and B), fostering a more cooperative microbial assemblage. Enhanced positive cohesion underpins more efficient C flow through trophic networks, as cooperative interactions reduce competition for limited substrates and facilitate the cross-feeding of metabolic byproducts. The connector keystone OTUs spanned multiple modules (Appendix D), suggesting that *B. velezensis* acts as a nexus, bridging indigenous taxa into cohesive functional guilds that expedite EOC mineralization. Finally, although *B. velezensis* effectively accelerates C mineralization, its focus on specific taxa reduces overall species richness, a trade-off that may affect long-term soil resilience. Combining *B. velezensis* with other microbial inoculants or physicochemical amendments could balance rapid functional recovery with biodiversity conservation. Accordingly, field trials under variable conditions are essential to validate these mechanisms and safeguard soil health.

Our results reveal a short-term trade-off, *B. velezensis* inoculation in DZ-fumigated soil reduced taxonomic richness while markedly increasing EOC mineralization. This pattern is consistent with dominance by a few highly efficient decomposers that accelerate immediate substrate turnover but simultaneously reduce functional redundancy, potentially lowering the community's buffering capacity against future disturbances (Chen *et al.* 2022). Consequently, rapid functional recovery may not equate to long-term resilience; soils dominated by specialist taxa may be more vulnerable to environmental fluctuations or subsequent stressors (Barnett and Shade 2024; de Mills *et al.* 2025). To manage this trade-off, we recommend strategies that combine targeted inoculants with diversity-supporting measures — for example, multi-strain consortia integrating decomposer specialists with generalist or keystone-support taxa, and organic amendments (e.g., biochar or compost) that enhance recolonization and habitat heterogeneity (Zhu *et al.* 2024; Zhou *et al.* 2026). Finally, we emphasize the need for field-scale, longitudinal studies to determine whether functional gains persist and whether taxonomic richness and redundancy recover over time, thereby ensuring that short-term remediation does not incur long-term ecosystem costs.

5. Conclusion

In this study, we demonstrated that: 1) chemical fumigation with dazomet (DZ) and dimethyl disulfide (DMDS) significantly suppresses exogenous organic carbon (EOC) mineralization by disrupting microbial diversity, community composition, and metabolic activity, and 2) inoculation with *B. velezensis* effectively counteracts these inhibitory effects in DZ-treated soils, fully restoring EOC mineralization rates and enhancing microbial respiration. Mechanistically, *B. velezensis* drives a targeted reassembly of the bacterial community, selectively enriching efficient decomposers (*Acidobacteriota*) and core species (OTU56: *Ferdinandcohnia*, OTU181: *Niallia*), while suppressing competing taxa such as *Pseudomonas*. Network analysis revealed that inoculation with *B. velezensis* increases co-occurrence complexity, positive inter-taxon correlations, and keystone connectivity, thereby fostering

a more cooperative and robust microbial consortium. Structural equation modeling confirmed that *B. velezensis* inoculation increased the contribution of microbial diversity to EOC mineralization. Our results underscore the potential of microbial inoculants for rapid soil function recovery post-fumigation. Future studies should combine *B. velezensis* with complementary biotic or physicochemical amendments and validate its performance under field conditions. This study advances our understanding of microbial ecological restoration and provides a blueprint for integrating biological amendments into sustainable soil health management following chemical fumigation.

Acknowledgements

This work was supported by the National Key Research and Development Program of China (2023YFD1701200), the Beijing Natural Science Foundation, China (6232034).

Declaration of competing interest

The authors declare that they have no conflict of interest.

Declaration of generative AI and AI-assisted technologies in the writing process

The authors declare that they did not use AI in the preparation and writing of this manuscript.

Appendices associated with this paper are available at https://doi.org/10.1016/j.jia.2025.12.076

References

Abs E, Chase A B, Manzoni S, Ciais P, Allison S D. 2024. Microbial evolution — An under-appreciated driver of soil carbon cycling. *Global Change Biology*, **30**, e17268.

Barnett S E, Shade A. 2024. Arrive and wait: Inactive bacterial taxa contribute to perceived soil microbiome resilience after a multidecadal press disturbance. *Ecology Letters*, **27**, e14393.

Bissett A, Brown M V, Siciliano S D, Thrall P H. 2013. Microbial community responses to anthropogenically induced environmental change: Towards a systems approach. *Ecology Letters*, **16**, 128–139.

Brookes P C, Landman A, Pruden G, Jenkinson D S. 1985. Chloroform fumigation and the release of soil nitrogen: A rapid direct extraction method to measure microbial biomass nitrogen in soil. *Soil Biology and Biochemistry*, **17**, 837–842.

Callahan B J, McMurdie P J, Rosen M J, Han A W, Johnson A J A, Holmes S P. 2016. DADA2: High-resolution sample inference from Illumina amplicon data. *Nature Methods*, **13**, 581–583.

Cao T, Luo Y, Shi M, Tian X, Kuzyakov Y. 2024. Microbial interactions for nutrient acquisition in soil: Miners, scavengers, and carriers. *Soil Biology and Biochemistry*, **188**, 109215.

Carini P, Marsden P J, Leff J W, Morgan E E, Strickland M S, Fierer N. 2016. Relic DNA is abundant in soil and obscures estimates of soil microbial diversity. *Nature Microbiology*, **2**, 1–6.

Castellano-Hinojosa A, Boyd N S, Strauss S L. 2022. Impact of fumigants on non-target soil microorganisms: A review. *Journal of Hazardous Materials*, **427**, 128149.

Chen H, Ma K, Lu M, Fu Q, Qiu Y, Zhao J, Huang Y, Yang Y, Schadt C W, Chen H. 2022. Functional redundancy in soil microbial community based on metagenomics across the globe. *Frontiers in Microbiology*, **13**, 878978.

Chen Y, Feng X, Zhao X, Hao X, Tong L, Wang S, Ding R, Kang S. 2025. Biochar application enhances soil quality by improving soil physical structure under particular water and salt conditions in arid region of Northwest China. *Journal of Integrative Agriculture*, **24**, 3242–3263.

Chowdhury S, Farrell M, Bolan N. 2014. Priming of soil organic carbon by malic acid addition is differentially affected by nutrient availability. *Soil Biology and Biochemistry*, **77**, 158–169.

Cui J, Zhu Z, Xu X, Liu S, Jones D L, Kuzyakov Y, Shibistova O, Wu J, Ge T. 2020. Carbon and nitrogen recycling from microbial necromass to cope with C:N stoichiometric imbalance by priming. *Soil Biology and Biochemistry*, **142**, 107720.

Deng X, Zhang N, Shen Z, Zhu C, Liu H, Xu Z, Li R, Shen Q, Salles J F. 2021. Soil microbiome manipulation triggers direct and possible indirect suppression against *Ralstonia solanacearum* and *Fusarium oxysporum*. *NPJ Biofilms and Microbiomes*, **7**, 33.

Dungan R S, Gan J, Yates S R. 2003. Accelerated degradation of methyl isothiocyanate in soil. *Water, Air, and Soil Pollution*, **142**, 299–310.

Fang W, Wang X, Huang B, Zhang D, Liu J, Zhu J, Yan D, Wang Q, Cao A, Han Q. 2020. Comparative analysis of the effects of five soil fumigants on the abundance of denitrifying microbes and changes in bacterial community composition. *Ecotoxicology and Environmental Safety*, **187**, 109850.

Ge T, Wei X, Razavi B S, Zhu Z, Hu Y, Kuzyakov Y, Jones D L, Wu J. 2017. Stability and dynamics of enzyme activity patterns in the rice rhizosphere: Effects of plant growth and temperature. *Soil Biology and Biochemistry*, **113**, 108–115.

Del Giorgio P A, Cole J J. 1998. Bacterial growth efficiency in natural aquatic systems. *Annual Review of Ecology and Systematics*, **29**, 503–541.

de Graaff M A, Adkins J, Kardol P, Throop H L. 2015. A meta-analysis of soil biodiversity impacts on the carbon cycle. *Soil*, **1**, 257–271.

Guo Z, Lu Z, Liu Z, Zhou W, Yang S, Lv J, Wei M. 2024. Difference in the effect of applying *Bacillus* to control tomato *Verticillium* wilt in black and red soil. *Microorganisms*, **12**, 797.

Hui C, Sun P, Guo X, Jiang H, Zhao Y, Xu L. 2018. Shifts in microbial community structure and soil nitrogen mineralization following short-term soil amendment with the ammonifier *Bacillus amyloliquefaciens* DT. *International Biodeterioration & Biodegradation*, **132**, 40–48.

Ibekwe A M, Papiernik S K, Gan J, Yates S R, Yang C H, Crowley D E. 2001. Impact of fumigants on soil microbial communities. *Applied and Environmental Microbiology*, **67**, 3245–3257.

Jiang Z, Vancov T, Fang Y, Tang C, Zhang W, Xiao M, Song X, Zhou J, Ge T, Cai Y. 2025. Sustained superiority of biochar over straw for enhancing soil biological-phosphorus via the mediation of *phoD*-harboring bacteria in subtropical Moso bamboo forests. *Forest Ecology and Management*, **584**, 122606.

Kalam S, Basu A, Ahmad I, Sayyed R, El-Enshasy H A, Dailin D J, Suriani N L. 2020. Recent understanding of soil Acidobacteria and their ecological significance: A critical review. *Frontiers in Microbiology*, **11**, 580024.

Li J, Song Z, Wang Y, Chen C, Jiang H, Ding T, Xie S. 2025. Root exudates mediate *Bacillus velezensis* FZB42's colonization-independent biocontrol in maize. *Journal of Agricultural and Food Chemistry*, **73**, 22.

Liang C, Schimel J P, Jastrow J D. 2017. The importance of anabolism in microbial control over soil carbon storage. *Nature Microbiology*, **2**, 17105.

Liang Y, Cao D, Ma Z, Wu R, Zhang H, Fang Y, Shahbaz M, Liu X J A, Kuzyakov Y, Chen J. 2024. Stoichiometry regulates rice straw-induced priming effect: The microbial life strategies. *Soil Biology and Biochemistry*, **196**, 109514.

Liu Q, Zhu Z, Wei L, Zhang W, Wang S, Yuan H, Chen J, Ge T, Xu M, Kuzyakov Y. 2025. Bacterial necromass decomposition and priming effects in paddy soils depend on long-term fertilization. *Soil Biology and Biochemistry*, **211**, 109992.

Malik A A, Puissant J, Buckeridge K M, Goodall T, Jehmlich N, Chowdhury S, Gweon H S, Peyton J M, Mason K E, van Agtmaal M. 2018. Land use driven change in soil pH affects microbial carbon cycling processes. *Nature Communications*, **9**, 3591.

Mawarda P C, Lakke S L, van Elsas J D, Salles J F. 2022. Temporal dynamics of the soil bacterial community following *Bacillus* invasion. *iScience*, **25**, 104029.

de Mills S, Ijaz U Z, Lens P N L. 2025. Environmental instability reduces shock resistance by enriching specialist taxa with distinct two component regulatory systems. *NPJ Biofilms and Microbiomes*, **11**, 54.

Mosela M, Andrade G, Massucato L, de Araújo Almeida S, Nogueira A, de Lima Filho R, Zeffa D, Mian S, Higashi A, Shimizu G. 2022. *Bacillus velezensis* strain Ag75 as a new multifunctional agent for biocontrol, phosphate solubilization and growth promotion in maize

and soybean crops. *Scientific Reports*, **12**, 15284.
Nielsen U N, Ayres E, Wall D H, Bardgett R D. 2011. Soil biodiversity and carbon cycling: A review and synthesis of studies examining diversity–function relationships. *European Journal of Soil Science*, **62**, 105–116.
Pan T, Chen Y, Li S, Wang L, Muramoto J, Shennan C, Tian J, Cai K. 2025. Anaerobic soil disinfestation rather than *Bacillus velezensis* Y6 inoculant suppresses tomato bacterial wilt by improving soil quality and manipulating bacterial communities. *Journal of Integrative Agriculture*, **24**, 754–768.
Philippot L, Chenu C, Kappler A, Rillig M C, Fierer N. 2024. The interplay between microbial communities and soil properties. *Nature Reviews Microbiology*, **22**, 226–239.
Prider J, Williams A. 2014. Using dazomet to reduce broomrape seed banks in soils with low moisture content. *Crop Protection*, **59**, 43–50.
Qiao Y, Wang T, Huang Q, Guo H, Zhang H, Xu Q, Shen Q, Ling N. 2024. Core species impact plant health by enhancing soil microbial cooperation and network complexity during community coalescence. *Soil Biology and Biochemistry*, **188**, 109231.
Quast C, Pruesse E, Yilmaz P, Gerken J, Schweer T, Yarza P, Peplies J, Glöckner F O. 2012. The SILVA ribosomal RNA gene database project: Improved data processing and web-based tools. *Nucleic Acids Research*, **41**, D590–D596.
Wu R, Zhang Z, Li G, Wang X, Fang Y, Kuzyakov Y, Xu X, Chen J, Ge T, Zhu Z. 2026. Frequency and C:N:P stoichiometry of organic inputs determines intensity of net C balance in paddy soils. *Soil Biology and Biochemistry*, **214**, 110051.
Schulte-Uebbing L F, Beusen A H, Bouwman A F, De Vries W. 2022. From planetary to regional boundaries for agricultural nitrogen pollution. *Nature*, **610**, 507–512.
Sennett L B, Burton D L, Goyer C, Zebarth B J. 2022. Chemical fumigation alters soil carbon and nitrogen dynamics in soils amended with substrates of contrasting carbon availability. *Geoderma*, **419**, 115878.
Shu X, Hu Y, Liu W, Xia L, Zhang Y, Zhou W, Liu W, Zhang Y. 2023. Linking between soil properties, bacterial communities, enzyme activities, and soil organic carbon mineralization under ecological restoration in an alpine degraded grassland. *Frontiers in Microbiology*, **14**, 1131836.
Sinsabaugh R L, Follstad Shah J J. 2012. Ecoenzymatic stoichiometry and ecological theory. *Annual Review of Ecology*, *Evolution*, *and Systematics*, **43**, 313–343.
Sun X, Xu Z, Xie J, Hesselberg-Thomsen V, Tan T, Zheng D, Strube M L, Dragoš A, Shen Q. 2022. *Bacillus velezensis* stimulates resident rhizosphere *Pseudomonas stutzeri* for plant health through metabolic interactions. *ISME Journal*, **16**, 774–787.
Trabelsi D, Mhamdi R. 2013. Microbial inoculants and their impact on soil microbial communities: A review. *BioMed Research International*, **2013**, 863240.
Walters W, Hyde E R, Berg-Lyons D, Ackermann G, Humphrey G, Parada A, Gilbert J A, Jansson J K, Caporaso J G, Fuhrman J A. 2016. Improved bacterial 16S rRNA gene (V4 and V4-5) and fungal internal transcribed spacer marker gene primers for microbial community surveys. *mSystems*, **1**, e00009-16.
Wang C, Liu D, Bai E. 2018. Decreasing soil microbial diversity is associated with decreasing microbial biomass under nitrogen addition. *Soil Biology and Biochemistry*, **120**, 126–133.
Wei X, Ge T, Wu C, Wang S, Mason-Jones K, Li Y, Zhu Z, Hu Y, Liang C. 2021. T4-like phages reveal the potential role of viruses in soil organic matter mineralization. *Environmental Science & Technology*, **55**, 6440–6448.
Wu J, Pommerening B, Chaussod R, Brookes P. 1990. Measurement of soil microbial biomass C by fumigation-extraction-an automated procedure. *Soil Biology and Biochemistry*, **22**, 1167–1169.
Xiong J, Du L, Li N, Wu X, Xiang Y, Li S, Zou L, Liu D, Huang D, Xie Z F. 2024. Pigmentiphaga kullae CHJ604 improved the growth of tobacco by degrading allelochemicals and xenobiotics in continuous cropping obstacles. *Journal of Hazardous Materials*, **465**, 133466.
Yan D, Cao A, Wang Q, Li Y, Canbin O, Guo M, Guo X. 2019. Dimethyl disulfide (DMDS) as an effective soil fumigant against nematodes in China. *PLoS ONE*, **14**, e0224456.
Yan D, Liu J, Wang X, Fang W, Li Y, Cao A, Wang Q. 2025. A review on the mechanisms of fumigant action. *New Plant Protection*, **2**, e27.
Zargar A N, Lymperatou A, Skiadas I, Kumar M, Srivastava P. 2022. Structural and functional characterization of a novel biosurfactant from *Bacillus* sp. IITD106. *Journal of Hazardous Materials*, **423**, 127201.
Zegeye E K, Brislawn C J, Farris Y, Fansler S J, Hofmockel K S, Jansson J K, Wright A T, Graham E B, Naylor D, McClure R S. 2019. Selection, succession, and stabilization of soil microbial consortia. *mSystems*, **4**, e00055-19.
Zhao Y, Guan D, Liu X, Gao G F, Meng F, Liu B, Xing P, Jiang X, Ma M, Cao F. 2022. Profound change in soil microbial assembly process and co-occurrence pattern in co-inoculation of *Bradyrhizobium japonicum* 5038 and *Bacillus aryabhattai* MB35–5 on soybean. *Frontiers in Microbiology*, **13**, 846359.
Zhou J S, Tang C X, Vancov T, Fu S L, Fang Y Y, Ge T D, Dong Y F, Luo Y, Yu B, Cai Y J, White J C, Li Y F. 2026. Biochar mitigates the suppressive effects of nitrogen deposition on soil methane uptake in a subtropical forest. *Agriculture*, *Ecosystems & Environment*, **395**, 109951.
Zhu X, Li Y, Wang H, Zhang L. 2024. Biochar regulates the functions of keystone taxa to reduce *p*-coumaric acid accumulation in soil. *Frontiers in Microbiology*, **15**, 1458185.
Zhu Z, Fang Y, Liang Y, Li Y, Liu S, Li Y, Li B, Gao W, Yuan H, Kuzyakov Y. 2022. Stoichiometric regulation of priming effects and soil carbon balance by microbial life strategies. *Soil Biology and Biochemistry*, **169**, 108669.
Zhu Z, Ge T, Luo Y, Liu S, Xu X, Tong C, Shibistova O, Guggenberger G, Wu J. 2018. Microbial stoichiometric flexibility regulates rice straw mineralization and its priming effect in paddy soil. *Soil Biology and Biochemistry*, **121**, 67–76.